ACCEPTED ARTICLE PREVIEW

Accepted Article Preview: Published ahead of advance online publication

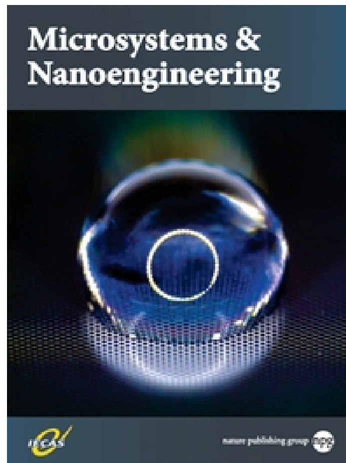

Precision micro-mechanical components in single crystal diamond by deep reactive ion etching

Adrien Toros, Marcell Kiss, Teodoro Graziosi, Hamed Sattari, Pascal Gallo and Niels Quack

Adrien Toros, Marcell Kiss, Teodoro Graziosi, Hamed Sattari, Pascal Gallo and Niels Quack. Precision micro-mechanical components in single crystal diamond by deep reactive ion etching. Microsystems & Nanoengineering accepted article preview 9 March 2018; doi: s41378-018-0014-5.

This is a PDF file of an unedited peer-reviewed manuscript that has been accepted for publication. NPG are providing this early version of the manuscript as a service to our customers. The manuscript will undergo copyediting, typesetting and a proof review before it is published in its final form. Please note that during the production process errors may be discovered which could affect the content, and all legal disclaimers apply.

Received 29 November 2017; accepted 9 March 2018

1 # Precision micro-mechanical components in single
2 crystal diamond by deep reactive ion etching

3 Running title : Micro-Mechanical Components in Single Crystal Diamond

4

5 Adrien Toros*, Marcell Kiss, Teodoro Graziosi, Hamed Sattari, Pascal Gallo and Niels
6 Quack*

7 Ecole Polytechnique Federale de Lausanne
8
9
10
11 Corresponding authors: * Adrien Toros, adrien.toros@epfl.ch
12 * Niels Quack, Email: niels.quack@epfl.ch

Microsystems & Nanoengineering

Abstract

The outstanding material properties of single crystal diamond have been at the origin of the long-standing interest in its exploitation for engineering of high performance micro- and nanosystems. In particular, the extreme mechanical hardness, the highest elastic modulus of any bulk material, low density and the promise for low friction have spurred interest most notably for micro-mechanical and MEMS applications. While reactive ion etching of diamond has been reported previously, precision structuring of freestanding micro-mechanical components in single crystal diamond by deep reactive ion etching has hitherto remained elusive, related to limitations in the etch processes, such as the need of thick hard masks, micro-masking effects and limited etch rates. In this work, we report on an optimized reactive ion etching process of single crystal diamond overcoming several of these shortcomings at the same time, and present a robust and reliable method to produce fully released micro-mechanical components in single crystal diamond. Using an optimized Al/SiO_2 hard mask and a high intensity oxygen plasma etch process, we obtain etch rates exceeding 30 µm/h and hard mask selectivity better than 1:50. We demonstrate fully freestanding micro-mechanical components for mechanical watches made of pure single crystal diamond. The components with a thickness of 150 µm are defined by lithography and deep reactive ion etching, and exhibit sidewall angles of 82° to 93° with surface roughness better than 200 nm rms, demonstrating the potential of this powerful technique for precision microstructuring of single crystal diamond.

Keywords

Single crystal diamond, deep reactive ion etching, micro-mechanical components.

Introduction

In recent years, the growth of synthetic diamond crystals has been industrialized based on High Pressure High Temperature (HPHT) or Chemical Vapor Deposition (CVD) growth techniques[1,2]. Several suppliers provide today commercial offerings of high quality single

Microsystems & Nanoengineering

crystal diamond substrates, cut and polished to plates in the size of a few tens of square millimeters and up to several hundreds of microns thick (e.g. Element Six or LakeDiamond SA). Such plates are of uniform size and free from defects typically present in natural diamonds, which makes them ideal substrates for optical and mechanical components made entirely of single crystal diamond.

Traditional techniques for structuring of diamond crystals typically involve cutting and fine polishing[3]. While these techniques allow for flat surfaces of optically superb quality, they can be applied to curved structures and microstructures only to a limited extent. The most advanced technique for precision structuring of single crystal diamond today is ultrashort pulse laser microstructuring, which has recently been performed on such substrates and allows to produce up to 1.2 mm thick curved optical components with a precision of 10 µm and a surface roughness of 1 µm rms[4]. However, the dimensions of these substrates and their excellent uniformity also allows them to be processed using standard microfabrication techniques, which opens an entirely novel direction of processing methods and a potential for parallelization. Consequently, the availability of such substrates has led to a tremendous increase in interest in scientific and engineering research over the past decade, targeting to exploit the extraordinary optical, mechanical and thermal properties of this unique material.

Examples of recent demonstrations in single crystal diamond micro- and nanosystem engineering include mechanical systems such as high-Q nanomechanical resonators[5], extremely hard nanowire tips[6,7], nanoindenters[8] and stiff cantilevers[9], and optical components such as micro-lenses[10,11], gratings[12] and microcavities[13]. In these applications, single crystal diamond permits excellent performance compared to similar structures made in any other material. Enormous interest is further arising of the intriguing possibilities to include optically active defects, color-centers such as the nitrogen-vacancy complex, which have led to entirely novel applications, such as scanning diamond magnetometry[14,15], on-chip quantum information processing[16], labelling[17,18] and quantum cryptography[19,20] (for a recent review on diamond nanofabrication, see Reference 21).

Microsystems & Nanoengineering

1 Precision structuring of diamond has - in several of these demonstrations - been achieved
2 using microfabrication based on lithography and reactive ion etching. The advantages of
3 such a fabrication approach lie in the high resolution allowed by lithography, the possibility of
4 parallel fabrication, and the smooth surfaces[22] that can be obtained by reactive ion etching
5 processes.

6 For devices on the nanoscale range, electron beam lithography is routinely used to pattern e-
7 beam resists such as Hydrogen silsesquioxane (HSQ). Once patterned, these resists are
8 suitable etch masks for the reactive ion etching of diamond when limited etching depths are
9 required. Lončar et al.[23] have used this approach to fabricate single crystal diamond
10 nanowires of about 2 µm in height. For applications requiring deeper etching, structured
11 electron beam resists commonly serve as etch mask to pattern underlying metallic or
12 dielectric layers, which in turn serve as hard mask for the reactive ion etching of diamond to
13 achieve more important etch depths. Diamond nanoslabs were demonstrated by Englund et
14 al.[24] using ZEP electron beam resist to pattern a 80 nm thick chromium hard mask,
15 subsequently etching the diamond substrate 10 µm deep. Finally, patterned electron beam
16 resists are also suitable for lift-off processes. Gu et al.[25] obtained diamond pillars about 1 µm
17 tall by evaporating chromium on an electron beam patterned PMMA resist, followed by lift-off
18 and reactive ion etching of diamond. While these methods use electron beam lithography
19 and allow obtaining nanostructures, photolithography is an excellent alternative when the
20 desired critical dimensions are in the micrometer range. For instance, extensive
21 developments in the field of diamond micro-lenses have been reported, which generally are
22 based on photolithography and thermal reflow for patterning a photoresist layer. Wang et
23 al.[26] have recently demonstrated micro-lenses with diameters of about 15 µm and height of
24 about 300 nm. For such etching depths and similarly to electron beam resists, photoresists
25 are generally well suited as etch mask material during the reactive ion etching of diamond.
26 The vast majority of etching processes are based on oxygen plasma in combination with a
27 secondary gas. Pure oxygen plasma has been used by Degen et al.[27] to produce diamond

Microsystems & Nanoengineering

tips of a few micrometers in length, while Maletinsky et al.[28] use an argon/oxygen plasma to fabricate 2 µm long pillars on a thin diamond membrane, obtained beforehand with cycles of pure oxygen and argon/chlorine plasmas. Etching processes can further be tailored to specific requirements by modifying parameters such as the chamber pressure, the gas flows, the plasma and the bias power. These adjustments influence the directionality of the etching, the etched surface roughness, the etching rate and the selectivity to the hard mask. Etch rates up to 40 µm/h[29] and selectivity to the hard mask material up to 1:200 have previously been reached[30], however, structures etched into single crystal diamond have typically been limited to a thickness ranging from a few hundreds of nanometers to a few tens of microns. The highest hitherto reported etch depth amounts to 55 µm using a high-grade steel structure as a hard mask, positioned by pick-and-place on the diamond surface[31]. However, this approach does not benefit from the precision of photolithography techniques. To the best of our knowledge, the structure with the most important thickness realized in single crystal diamond by photolithography and reactive ion etching techniques is a 50 µm thick diamond probe recently demonstrated by Yacoby et al.[32] The structure is obtained by photolithography and a pure oxygen plasma with a titanium hard mask, subsequently mechanically released from the diamond substrate and attached to a tipless AFM cantilever. This thickness range is well suited for the fabrication of released diamond devices for applications such as cantilevers for atomic force microscopy; however, for micro-mechanical components such as required in time-keeping mechanisms in mechanical watches, there is a need for a minimum threefold increase in etch depth.

This limitation in etch depth arises from a combination of challenges associated to the requirements for deep reactive ion etch processes: in order to achieve high anisotropic etch rates and vertical etch profiles, typically high density plasmas with high platen bias power are required. While the high energy from the platen bias results in increased etch rate, the hard mask is equally subjected to high energy ion impacts. Thus, the hard mask is rapidly consumed, consequently a thick hard mask layer is required to achieve deep etching in

Microsystems & Nanoengineering

1 diamond. Furthermore, sputtering of the hard mask material with subsequent re-deposition
2 on the diamond surface can occur. With the re-deposited particles acting locally as hard
3 mask material, further etching is prevented at these locations and columnar whisker
4 structures are formed. This effect will result in rough surfaces[33] and will lead to slow down
5 and eventual stopping of the etch before reaching the bottom of the substrate. This
6 phenomenon is commonly referred to as micromasking, which intensifies with increasing
7 etch duration and plasma anisotropy[12], thus making it difficult to reach high etch depths. An
8 additional practical challenge is associated to the substrate size being limited to a few tens of
9 mm^2: when applying standard spin coating for photoresist deposition, edge bead formation of
10 the photoresist[34–36] will limit the resolution of the lithography process.

11 **Materials and Methods**

12 In this work, we have developed a method to overcome these limitations to reach
13 unprecedented depths in single crystalline diamond, allowing to completely etch through
14 diamond substrates and releasing lithographically defined components. The fabrication
15 process is shown schematically in Figure 1, and the detailed protocol is described in Section
16 I of the supplementary information.

17

Microsystems & Nanoengineering

1

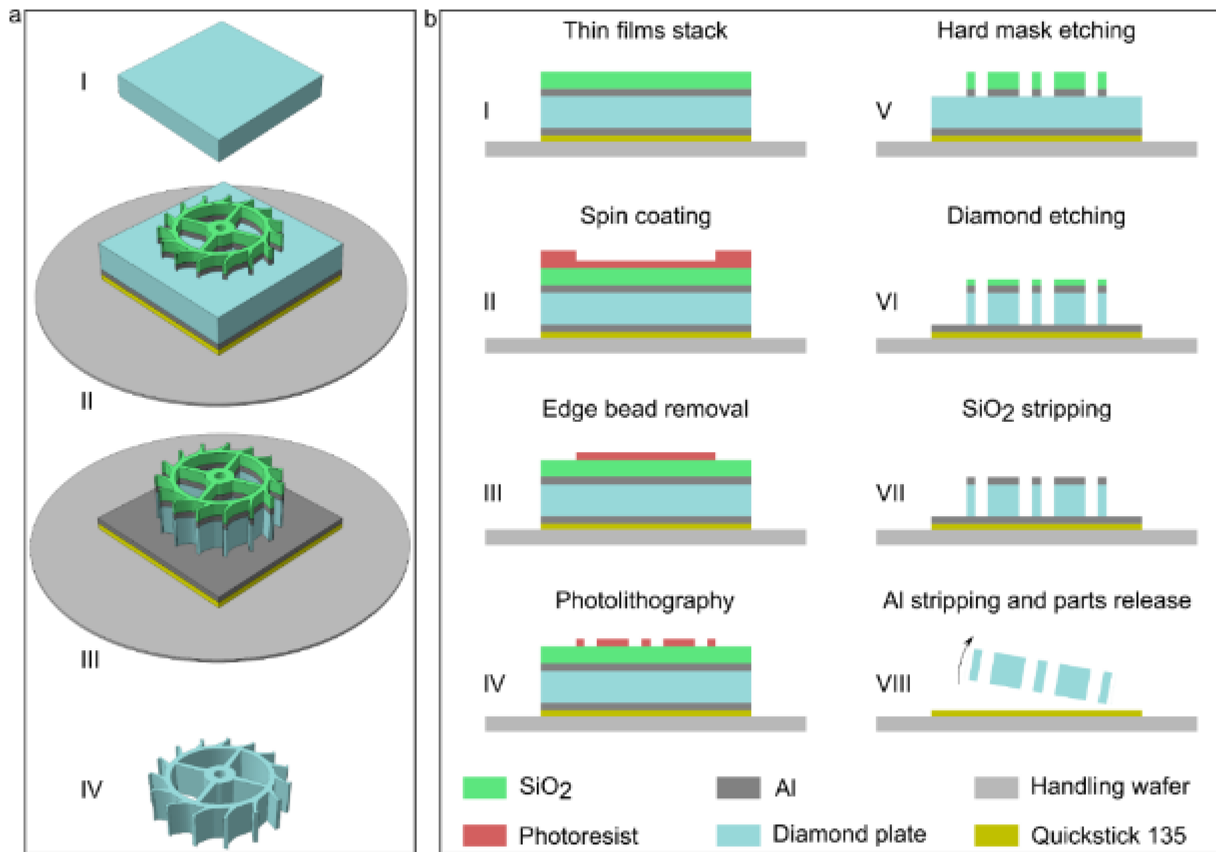

2 **Figure 1** (a) Schematic 3D representation of the main microfabrication process steps for the
3 fabrication of released components in single crystalline diamond. On the top surface of the initial 5.5
4 mm x 5.5 mm x 150 µm diamond substrate (step I), a thick SiO_2 hard mask on an Al adhesion layer is
5 patterned by photolithography and dry etching. A sacrificial Al layer is deposited on the diamond
6 backside and the stack is assembled on a handling wafer with a mounting wax (step II). The pattern is
7 transferred to the diamond by deep reactive ion etching (step III). Finally, the remaining hard mask and
8 the sacrificial Al layer on the bottom surface of the diamond are stripped to release the parts (step IV).
9 (b) Detailed cross section schematic of the microfabrication process steps for the fabrication of
10 released components in single crystalline diamond showing the thin films stack deposition (step I), the
11 photoresist spin coating with the edge bead formation (step II) and subsequent removal (step III), the
12 photolithography with the components patterns (step IV), the hard mask etching (step V), the diamond
13 deep reactive ion etching (step VI), the remaining hard mask stripping (step VII) and the Al stripping to
14 release the parts (step VIII).

15 In a first step, a suitable hard mask is deposited on the diamond substrate with a typical
16 dimension of 5.5 mm x 5.5 mm x 150 µm. Metal thin films such as aluminum have previously
17 been used as hard mask materials for single crystal diamond etching. They provide good
18 adhesion on diamond[36], and show good selectivity (~1:100)[30]. However, metal hard masks
19 generally result in significant micromasking during highly energetic oxygen plasma based
20 diamond etching[33,37]. In contrast, dielectric thin films of silicon oxide (SiO_2) or alumina (Al_2O_3)
21 have been used previously with minimum micromasking effects in pure oxygen plasmas[30]. In
22 this work, several hard mask materials (Al, Si, Al_2O_3, SiO_2) were experimentally assessed
23 using various plasma parameters and compositions. A pure oxygen plasma combined with a

Microsystems & Nanoengineering

1 SiO_2 hard mask strongly reduced micromasking effects while exhibiting a high etch rate and
2 a good selectivity to the diamond. However, challenges arose from the thick layer of hard
3 mask needed to etch through the diamond and the low adhesion of silicon oxide layers on
4 diamond[36].

5 With the oxygen plasma parameters and the SiO_2 hard mask used in our process, a
6 selectivity of 1:50 was measured. This would require a 3 µm thick SiO_2 hard mask to etch
7 through a 150 µm thick diamond plate. However, when using a highly biased plasma, hard
8 mask faceting is a commonly encountered issue that leads to angled sidewalls in the etched
9 substrate[38]. A well-known method used to minimize the effects of the hard mask faceting is to
10 use a hard mask thicker than required. In our process, a 7 µm thick hard mask is used, which
11 is much thicker than usually encountered in common microfabrication processes. This poses
12 a number of challenges in terms of mask adhesion and quality, but also in terms of mask
13 patterning: the low adhesion can result in delamination of the hard mask layer during
14 lithography[36] or when exposed to the plasma. Moreover, SiO_2 layers with such thicknesses
15 are generally highly susceptible to cracking due to the large internal stress[39]. To avoid the
16 mask from delaminating during the photolithography (specifically when the photomask is
17 removed from the photoresist coated diamond substrate surface after the exposure, or during
18 the development of the photoresist), an adhesion layer is needed between the diamond and
19 the hard mask. Chromium or titanium are typical adhesion layer materials, however in our
20 process, a 200 nm thick Al layer resulted in optimum adhesion of the hard mask to the
21 diamond substrate. In addition, an identical Al layer was deposited on the backside of the
22 diamond plate. This sacrificial layer is used for the removal of the etched components when
23 the diamond through etch is completed.

24 The SiO_2 hard mask was deposited by RF sputtering. Sputtering in Ar with added O_2 is
25 beneficial for decreasing the stress and the roughness in the film, while increasing its
26 hardness and adhesion[40]. However, the addition of O_2 also leads to a very slow deposition
27 rate, around 5 times slower than when using only Ar. Therefore, a first thin (65 nm) layer of

Microsystems & Nanoengineering

1 SiO_2 was deposited with both Ar and O_2 flow, while the remaining 7 µm layer was deposited
2 without added O_2 to obtain an increased deposition rate. The thin layer deposited under
3 oxygen flow acts effectively as a buffer layer between the Al and the SiO_2 layer deposited
4 without oxygen.

5 For patterning the hard mask, the diamond plate was temporarily attached to a 4-inch
6 handling Si wafer with a mounting wax to allow compatibility with standard microfabrication
7 tools (Figure 1b, step I). A 2.5 µm thick layer of photoresist was spin coated on the diamond
8 plate surface, which leads to an important edge bead (Figure 1b, step II) that has to be
9 removed, in order to have a close contact between the photomask and the photoresist during
10 exposure for high-resolution pattern transfer. Several solutions have previously been
11 employed for edge-bead reduction or removal, including equalizing height[35,41], in hole
12 placement[42,43], mask pick and place[44] and stamp-transfer[37,45]. We here developed a two
13 cycle photolithography exposure approach to completely remove the edge-bead region on
14 the small substrate (Section II of supplementary information). After the photoresist spin
15 coating, a first exposure is performed on a 0.5 mm wide frame covering the inside of the 4
16 edges of the diamond plate, with a high dose adapted to the important thickness of the edge
17 bead. In a subsequent first development (Section III of supplementary information), the edge
18 bead is removed (Figure 1b, step III) and allows to perform a closely contacted exposure of
19 the central region using a photomask with the components pattern. A second development
20 completes the photolithography process (Figure 1b, step IV) and is followed by the dry
21 etching of the SiO_2 hard mask, a short dip in buffered HF to smoothen the SiO_2 sidewalls
22 (Section IV of supplementary information), and the dry etching of the Al adhesion layer
23 (Figure 1b, step V). It is essential to perform the SiO_2 hard mask etching by iterating reactive
24 ion etch and cool-down steps, as the thermal conductance between the photoresist layer and
25 the cooled substrate holder is lowered by the wafer-adhesive-diamond stack. Without cool-
26 down between etching steps, the photoresist will overheat and disintegrate before the
27 completion of the hard mask etch. This microfabrication process flow using a hard mask

Microsystems & Nanoengineering

layer stack of 200 nm Al and 7 μm SiO_2, and a 2-cycle photolithography for edge bead removal, resulted in well resolved and defect free hard mask layers on 5.5 mm x 5.5 mm x 150 μm single crystal diamond substrates, as shown in Figure 2a and Figure 2b.

The diamond etching (Section V of supplementary information) is performed in an inductively coupled plasma (ICP) module (Figure 1b, step VI), and is followed by the remaining SiO_2 hard mask stripping (Figure 1b, step VII) and sacrificial Al stripping to release the parts (Figure 1b, step VIII). While initial experiments with Al hard masks resulted in excessive micromasking after 4 hours of Ar/O_2 based reactive ion etching (Figure 2c), this effect was strongly reduced by the use of the SiO_2 hard mask (Figure 2d), and 150 μm thick diamond substrates could be fully etched through after 5 hours O_2 reactive ion etch.

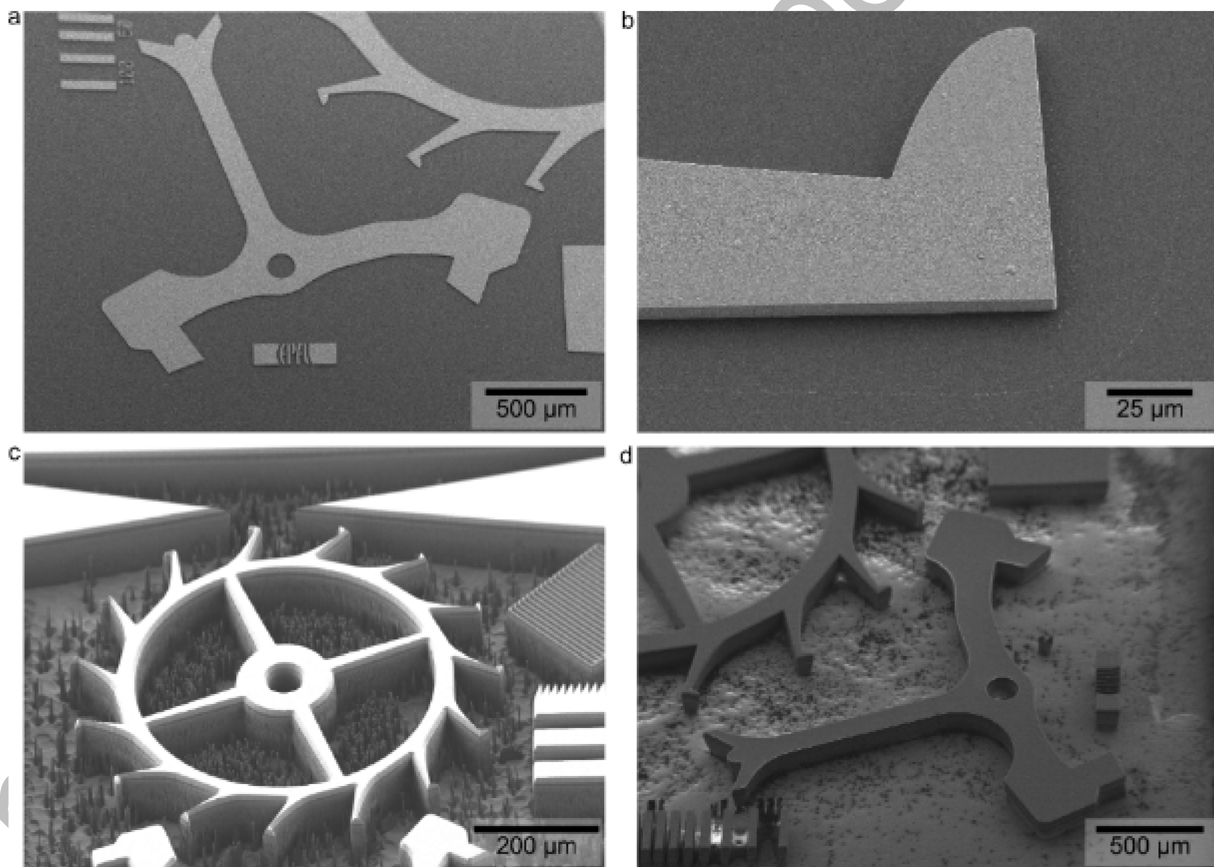

Figure 2 (a) High quality thin film hard mask layer stacks (200 nm Al, 7 μm SiO_2) deposited on diamond with (b) high resolution patterns. While initial experiments with Al hard masks resulted in (c) strong micromasking after 4 hours of Ar/O_2 reactive ion etching, this effect was (d) strongly reduced by the use of the SiO_2 hard mask, and 150 μm thick diamond substrates could be fully etched through after 5 hours O_2 reactive ion etch.

1 **Results and discussion**

2 In order to demonstrate the capabilities of the microfabrication process, we chose to
3 manufacture mechanical parts that are central components in time keeping mechanisms of
4 mechanical watches, including escape wheel and anchor. Nevertheless, the process is
5 suitable for the fabrication of a wide range of possible components, such as hairsprings,
6 nanoindenters, mechanical tips, diamond blades, optical components, etc. The application
7 for mechanical watches is a domain of particular interest, since the material properties of
8 single crystalline diamond can provide low weight components, high energy storage,
9 extremely low coefficient of friction[46], amagnetic mechanisms and attractive visual appeal.
10 The application typically requires micrometer dimensional tolerances with low sidewall
11 roughness. Figure 3a shows a photograph of two fabricated components, an escape wheel
12 and corresponding anchor. The yellow hue originates from nitrogen impurities in the
13 particular HPHT single crystalline diamond substrate that was used for the process. It is
14 possible to obtain colorless components or fancy colors (e.g. blue or pink) by using CVD
15 diamond, with a high level of purity or by deliberately adding specific impurities during growth
16 or irradiating the substrate after growth. Figure 3b shows a Scanning Electron Microscope
17 (SEM) recording of the escape wheel. The image reveals the precise definition of fine
18 features and good verticality of the sidewalls.

19

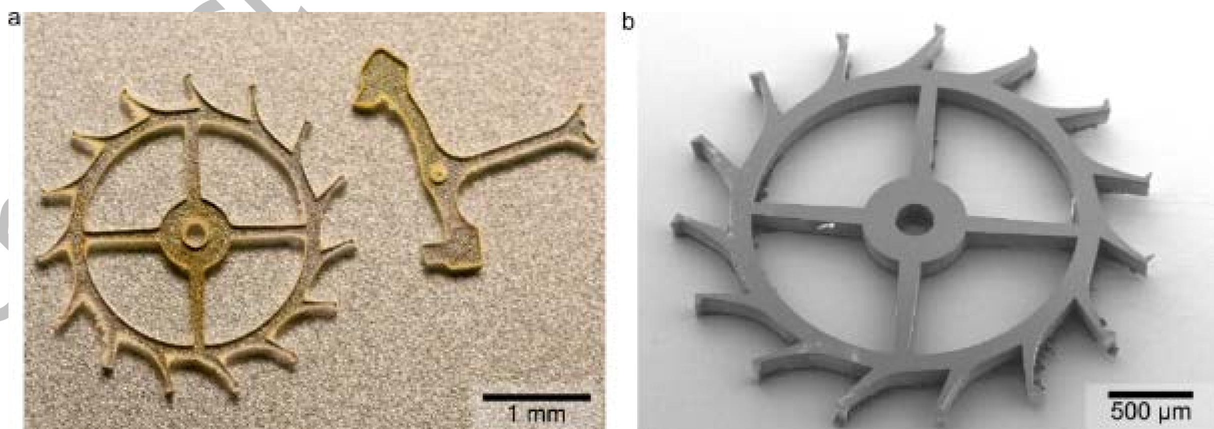

20

21 **Figure 3** (a) Photograph of a 150 μm thick escape wheel and anchor, obtained from a single crystal
22 diamond by deep reactive ion etching. (b) Scanning Electron Microscope recording of the escape
23 wheel, highlighting the unprecedented precision of the single crystal diamond component as a result
24 from the microfabrication process.

Microsystems & Nanoengineering

Based on optical microscope inspection, patterns measured on the diamond part top surface were laterally reduced on each edge by 5.7 μm (i.e. total reduction of 11.4 μm) in size compared to the original photomask design. This reduction in feature size is resulting from a combination of contact lithography and hard mask recess during the etch process, and can be further reduced by including an appropriate mask bias[30].

The profile of the sidewall (Figure 4a) is composed of two distinct regions. The bottom region (extending to about 125 μm from the bottom edge) exhibits a negative tapered (i.e. "retrograde") profile and an angle of 82.0°±1.4°, while the top region (extending to about 25 μm from the top edge) shows a positive tapered profile and a 93.4°±2.7° angle. The angle measurement method is described in Section VI of the supplementary information. The positive profile of the top region originates from the hard mask recess during the etching[47], while we attribute the origin of the bottom region negative profile to an isotropic component of the plasma characteristics, which can be further optimized by adjusting the plasma etch parameters.

While this sidewall profile can already prove sufficient for mechanical watch components, we expect that the verticality can further be improved by adjusting the combination of process pressure and bias power. Similar optimizations have been demonstrated in single crystal diamond for etch depths of up to 10 μm, where sidewall angles of 88.45° have been achieved by using periodical renewing of the hard mask during the etch[37]. Alternative approaches for sidewall verticality improvement can include cyclic passivation of the sidewalls as known from silicon deep reactive ion etching (Bosch process). In silicon, sidewall angles of 89.7° have been demonstrated for similar etching depths of 130 μm[48]. Such quasi-ideal sidewall angles are obtained by adjusting the etching time to passivation time ratio[49]. While similarly robust sidewall passivation techniques have not yet been developed for the deep etching of diamond, possible routes for sidewall passivation mechanisms for diamond etching can include controlled re-deposition using Ni or Ni-Ti alloy hard masks[50].

Microsystems & Nanoengineering

1 The sidewall roughness of the components was measured by Atomic Force Microscopy
2 (AFM). Figure 4b shows a SEM recording of the inspected sidewall, and the corresponding
3 AFM measurements for two selected sites in Figure 4c and 4d. The top region of the sidewall
4 exhibits a surface roughness as low as 20 nm (rms), while the bottom region shows a
5 surface roughness of about 200 nm (rms). These values correspond to the standard
6 deviation of the height in 5 µm x 5 µm areas, after plane fitting (i.e. data centering and tilt
7 removal). We attribute the two regions of different roughness to the different profiles of the
8 top and bottom region of the sidewall. While the bottom region retains striations caused by
9 the original hard mask sidewalls roughness, the top region is submitted to a continuous
10 smoothening as the etch progresses. This top region smoothening effect is in agreement with
11 previous reports on reactive ion etching of diamond[47].

12 The surface quality obtained with our deep reactive ion etching process constitutes an
13 improvement of >5x (200 nm rms region) and >50x (20 nm rms region) compared to surface
14 roughness reported on sidewalls of 1.2 mm single crystalline diamond components obtained
15 by femtosecond laser structuring[4]. For much lower etch depths of up to 1 µm, previous
16 reports have shown even smoother sidewalls in single crystal diamond by reactive ion
17 etching[51], with peak-to-peak values of 10 - 20 nm (here: 400 – 800 nm), opening an avenue
18 for further improvement of the surface roughness.

19 While mechanical components will benefit from reduced friction, the reduction in surface
20 roughness opens further possibilities to manufacture optical components such as lenses,
21 gratings, prisms, filters or optical windows.

Microsystems & Nanoengineering

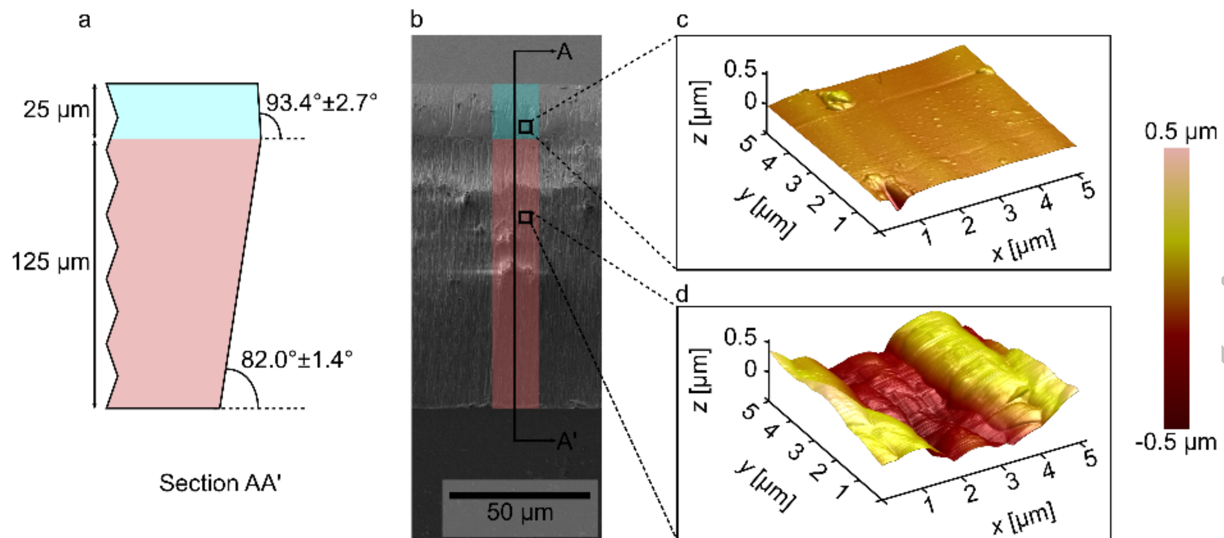

1

2 **Figure 4** (a) Schematic cross-sectional view of the released parts' sidewalls. (b) Scanning Electron
3 Microscope recording of a sidewall after deep reactive ion etch, revealing two distinct regions
4 separated at 25 µm from the top edge. Atomic Force Microscope measurements show a (c) surface
5 roughness as low as 20 nm rms in the top region, while (d) the bottom region exhibits a surface
6 roughness of 200 nm rms. The variation in roughness can be attributed to the different sidewall
7 profiles in the top and the bottom region.

8

9 Conclusion

10 In conclusion, we have for the first time demonstrated fully released precision micro-
11 mechanical components in 150 µm thick single crystalline diamond, obtained by deep
12 reactive ion etching. Prototypes of escape wheels and anchors for mechanical watches were
13 successfully fabricated. Commonly encountered challenges in deep reactive ion etching of
14 diamond were overcome by an optimized hard mask deposition and patterning process in
15 combination with a high density oxygen plasma etch with high bias power, avoiding
16 micromasking while obtaining high etch rate (30 µm/h) and high selectivity to the hard mask
17 (1:50) at the same time. The hard mask consists of a 3-layer stack to provide a well adhering
18 and defect free thick hard mask for complete diamond through etch. An Al adhesion layer
19 avoids the cracking or delamination of the thick SiO_2 hard mask, which is deposited in two
20 steps. In addition, a two-step photolithography procedure was used as effective photoresist
21 edge bead removal method, allowing for a high fidelity photolithography process. A sacrificial
22 Al layer between the diamond and the handling wafer allows for a simple release of the
23 fabricated components when the etching is completed. The characterization of the fabricated

Microsystems & Nanoengineering

parts revealed sidewalls angles of 82° to 93° and sidewalls roughness of better than 200 nm rms, at least 5x better than surface roughness obtained with traditional ultrashort pulse laser microstructuring techniques. This novel fabrication method is fully compatible with standard thin film deposition techniques, and photolithography allows to define arbitrarily shaped components for novel designs and geometries with high yield and high resolution. While the size of currently available single crystal diamond substrates is still limited, the process allows for parallelization of the critical fabrication steps, including etching and release, by multi-chip placement on a single carrier wafer, providing a route for volume production of lithographically defined precision micro-mechanical components.

Acknowledgments

The authors acknowledge funding by the Swiss National Science Foundation under grant No. 157566 and by the Gebert Rüf Stiftung under Grant No. GRS-043/16. The project is supported by LakeDiamond SA, a Swiss commercial supplier of cut and polished high purity single crystal diamond substrates. The designs for escape wheel and anchor have been adapted under CC-SA-4.0 from User:Fred the Oyster, Wikimedia Commons. All microfabrication steps were performed at the Center for Micro- and Nanofabrication CMi at EPFL. The authors gratefully acknowledge the technical support of the CMi management and staff.

Competing interests

P.G. is CEO and co-founder of LakeDiamond SA, a commercial supplier of the single crystal diamond samples used for this work. All other authors declare no conflict of interest.

Supplementary information

Supplementary information accompanies the manuscript on the Microsystems & Nanoengineering website (http://www.nature.com/micronano).

Microsystems & Nanoengineering

1 **References**

2 1 Schwander M, Partes K. A review of diamond synthesis by CVD processes. *Diam Relat*
3 *Mater* 2011; **20**: 1287–1301.

4 2 Gracio JJ, Fan QH, Madaleno JC. Diamond growth by chemical vapour deposition. *J*
5 *Phys Appl Phys* 2010; **43**: 374017.

6 3 Mildren R, Rabeau J. Optical Engineering of Diamond. Weinheim: Wiley-VCH, 2013.

7 4 Polikarpov M, Polikarpov V, Snigireva I *et al.* Diamond X-ray Refractive Lenses with High
8 Acceptance. *Phys Procedia* 2016; **84**: 213–220.

9 5 Tao Y, Boss JM, Moores BA *et al.* Single-crystal diamond nanomechanical resonators
10 with quality factors exceeding one million. *Nat Commun* 2014; **5**: 3638.

11 6 Tao Y, Degen CL. Single-Crystal Diamond Nanowire Tips for Ultrasensitive Force
12 Microscopy. *Nano Lett* 2015; **15**: 7893–7897.

13 7 Hausmann BJM, Khan M, Zhang Y *et al.* Fabrication of diamond nanowires for quantum
14 information processing applications. *Diam Relat Mater* 2010; **19**: 621–629.

15 8 Wheeler JM, Michler J. Invited Article: Indenter materials for high temperature
16 nanoindentation. *Rev Sci Instrum* 2013; **84**: 101301.

17 9 Fu J, Wang F, Zhu T *et al.* Single crystal diamond cantilever for micro-electromechanical
18 systems. *Diam Relat Mater* 2017; **73**: 267–272.

19 10 Lee CL, Gu E, Dawson MD *et al.* Etching and micro-optics fabrication in diamond using
20 chlorine-based inductively-coupled plasma. *Diam Relat Mater* 2008; **17**: 1292–1296.

21 11 Zhu T-F, Fu J, Wang W *et al.* Fabrication of diamond microlenses by chemical reflow
22 method. *Opt Express* 2017; **25**: 1185.

23 12 Forsberg P, Karlsson M. High aspect ratio optical gratings in diamond. *Diam Relat Mater*
24 2013; **34**: 19–24.

25 13 Khanaliloo B, Mitchell M, Hryciw AC *et al.* High- *Q* / *V* Monolithic Diamond Microdisks
26 Fabricated with Quasi-isotropic Etching. *Nano Lett* 2015; **15**: 5131–5136.

27 14 Maletinsky P, Hong S, Grinolds MS *et al.* A robust scanning diamond sensor for
28 nanoscale imaging with single nitrogen-vacancy centres. *Nat Nanotechnol* 2012; **7**: 320–
29 324.

30 15 Appel P, Neu E, Ganzhorn M *et al.* Fabrication of all diamond scanning probes for
31 nanoscale magnetometry. *Rev Sci Instrum* 2016; **87**: 063703.

32 16 Schröder T, Mouradian SL, Zheng J *et al.* Quantum nanophotonics in diamond [Invited].
33 *J Opt Soc Am B* 2016; **33**: B65–B83.

34 17 Schrand A, Hens SAC, Shenderova O. Nanodiamond Particles: Properties and
35 Perspectives for Bioapplications. *Crit Rev Solid State Mater Sci* 2009; **34**: 18–74.

36 18 Fu C-C, Lee H-Y, Chen K *et al.* Characterization and application of single fluorescent
37 nanodiamonds as cellular biomarkers. *Proc Natl Acad Sci* 2007; **104**: 727–732.

Microsystems & Nanoengineering

19 Beveratos A, Brouri R, Gacoin T *et al.* Single Photon Quantum Cryptography. *Phys Rev Lett* 2002; **89**: 187901.

20 Babinec TM, Hausmann BJM, Khan M *et al.* A diamond nanowire single-photon source. *Nat Nanotechnol* 2010; **5**: 195–199.

21 Castelletto S, Rosa L, Blackledge J *et al.* Advances in diamond nanofabrication for ultrasensitive devices. *Microsyst Nanoeng* 2017; **3**: 17061.

22 Enlund J, Isberg J, Karlsson M *et al.* Anisotropic dry etching of boron doped single crystal CVD diamond. *Carbon* 2005; **43**: 1839–1842.

23 Hausmann BJM, Khan M, Zhang Y *et al.* Fabrication of diamond nanowires for quantum information processing applications. *Diam Relat Mater* 2010; **19**: 621–629.

24 Hodges JS, Li L, Lu M *et al.* Long-lived NV^- spin coherence in high-purity diamond membranes. *New J Phys* 2012; **14**: 093004.

25 Jiang Q, Li W, Tang C *et al.* Large scale fabrication of nitrogen vacancy-embedded diamond nanostructures for single-photon source applications. *Chin Phys B* 2016; **25**: 118105.

26 Zhu T-F, Liu Z, Liu Z *et al.* Fabrication of monolithic diamond photodetector with microlenses. *Opt Express* 2017; **25**: 31586.

27 Tao Y, Degen CL. Single-Crystal Diamond Nanowire Tips for Ultrasensitive Force Microscopy. *Nano Lett* 2015; **15**: 7893–7897.

28 Appel P, Neu E, Ganzhorn M *et al.* Fabrication of all diamond scanning probes for nanoscale magnetometry. *Rev Sci Instrum* 2016; **87**: 063703.

29 Hwang DS, Saito T, Fujimori N. New etching process for device fabrication using diamond. *Diam Relat Mater* 2004; **13**: 2207–2210.

30 Chang KK. *Scanning Magnetometry with NV Centers in Diamond*. ETH Zürich (Doctoral Thesis No. 23962): Zürich, 2016.

31 Otterbach R. *Tiefenätzung in Diamant am Beispiel eines Drucksensors für Hochtemperaturanwendungen*. VDI Verlag: Düsseldorf, 2004.

32 Zhou TX, Stöhr RJ, Yacoby A. Scanning diamond NV center probes compatible with conventional AFM technology. *Appl Phys Lett* 2017; **111**: 163106.

33 Ando Y, Nishibayashi Y, Kobashi K *et al.* Smooth and high-rate reactive ion etching of diamond. *Diam Relat Mater* 2002; **11**: 824–827.

34 Forsberg P. *Diamond microfabrication for applications in optics and chemical sensing*. Acta Universitatis Upsaliensis: Uppsala, 2013.

35 Liu H, Reilly S, Herrnsdorf J *et al.* Large radius of curvature micro-lenses on single crystal diamond for application in monolithic diamond Raman lasers. *Diam Relat Mater* 2016; **65**: 37–41.

36 Otterbach R, Hilleringmann U, Horstmann TJ *et al.* Structures with a minimum feature size of less than 100 nm in CVD-diamond for sensor applications. *Diam Relat Mater* 2001; **10**: 511–514.

Microsystems & Nanoengineering

1 37 Vargas Catalan E, Forsberg P, Absil O *et al.* Controlling the profile of high aspect ratio
2 gratings in diamond. *Diam Relat Mater* 2016; **63**: 60–68.

3 38 Madou MJ. Fundamentals of Microfabrication: the Science of Miniaturization. 2nd ed.
4 Boca Raton: CRC press, 2002.

5 39 Zhang X, Chen K-S, Spearing SM. Residual stress and fracture of thick dielectric films for
6 power MEMS applications. In: *Technical Digest of The Fifteenth IEEE International*
7 *Conference on Micro Electro Mechanical Systems*. January 20-24, 2002, Las Vegas, NV,
8 USA, pp 164–167.

9 40 Fujiyama H, Sumomogi T, Endo T. Effect of O2 gas partial pressure on mechanical
10 properties of SiO2 films deposited by radio frequency magnetron sputtering. *J Vac Sci*
11 *Technol Vac Surf Films* 2002; **20**: 356–361.

12 41 Kehayias P, Jarmola A, Mosavian N *et al.* Solution nuclear magnetic resonance
13 spectroscopy on a nanostructured diamond chip. *Nat Commun* 2017; **8**: 188.

14 42 Otterbach R, Hilleringmann U, Goser K. Reactive ion etching of CVD-diamond for sensor
15 devices with a minimum feature size of 100 nm. In: *2000 26th Annual Conference of the*
16 *IEEE Industrial Electronics Society*. October 22-28, 2000. Nagoya, Japan, pp 1873–1877.

17 43 Shahrabi E, Sandrini J, Attarimashalkoubeh B *et al.* Chip-level CMOS co-integration of
18 ReRAM-based non-volatile memories. In: *2016 12th Conference on Ph.D. Research in*
19 *Microelectronics and Electronics (PRIME)*. June 27-30, 2016. Lisbon, Portugal, pp 1–4.

20 44 Li L, Bayn I, Lu M *et al.* Nanofabrication on unconventional substrates using transferred
21 hard masks. *Sci Rep* 2015; **5**: 7802.

22 45 Scheerlinck S, Dubruel P, Bienstman P *et al.* Metal Grating Patterning on Fiber Facets by
23 UV-Based Nano Imprint and Transfer Lithography Using Optical Alignment. *J Light*
24 *Technol* 2009; **27**: 1415–1420.

25 46 Chandrasekar S, Farris TN, Bhushan B. Ceramics for Magnetic Recording Applications.
26 In: *Friction and wear of ceramics*. New York: M. Dekker, 1994: 383-424.

27 47 Forsberg P, Karlsson M. Inclined surfaces in diamond: broadband antireflective
28 structures and coupling light through waveguides. *Opt Express* 2013; **21**: 2693–2700.

29 48 Lips B, Puers R. Three step deep reactive ion etch for high density trench etching. *J*
30 *Phys Conf Ser* 2016; **757**: 012005.

31 49 Wu B, Kumar A, Pamarthy S. High aspect ratio silicon etch: A review. *J Appl Phys* 2010;
32 **108**: 051101.

33 50 Ding GF, Mao HP, Cai YL *et al.* Micromachining of CVD diamond by RIE for MEMS
34 applications. *Diam Relat Mater* 2005; **14**: 1543–1548.

35 51 Hiscocks MP, Kaalund CJ, Ladouceur F *et al.* Reactive ion etching of waveguide
36 structures in diamond. *Diam Relat Mater* 2008; **17**: 1831–1834.

Microsystems & Nanoengineering